Journal of Molecular Structure 1163 (2018) 41–53

Contents lists available at ScienceDirect

Journal of Molecular Structure

journal homepage: http://www.elsevier.com/locate/molstruc

Evaluating structures, properties and vibrational and electronic spectra of the potassium 2-isonicotinoyltrifluoroborate salt

Maximiliano A. Iramain [a], Lilian Davies [b], Silvia Antonia Brandán [a, *]

[a] Cátedra de Química General, Instituto de Química Inorgánica, Facultad de Bioquímica, Química y Farmacia, Universidad Nacional de Tucumán, Ayacucho 471, 4000 San Miguel de Tucumán, Tucumán, Argentina
[b] Instituto de Investigaciones para la Industria Química (INIQUI, CONICET), Universidad Nacional de Salta, Av. Bolivia 5150, 4400 Salta, Argentina

ARTICLE INFO

Article history:
Received 7 November 2017
Received in revised form
19 February 2018
Accepted 26 February 2018
Available online 27 February 2018

Keywords:
Potassium 2-isonicotinoyltrifluorborate salt
Vibrational spectra
Molecular structure
Force field
DFT calculations

ABSTRACT

The potassium 2-isonicotinoyltrifluorborate salt has been characterized by using FT-IR, FT-Raman and UV−Visible spectroscopies while its structural properties were studied by using B3LYP/6-31G* and B3LYP/6-311++G** calculations in gas and aqueous solution phases. Four conformers with C_S and C_1 symmetries were found in the potential energy surfaces but only one of them presents the minimum energy. Two dimeric species of this salt were also optimized in accordance to the layered architectures suggested for trifluoroborate potassium salts in the solid phase. Here, the experimental Raman bands at 796, 748 and 676 cm^{-1} clearly support the presence of both dimers. On the other hand, the 2-isonicotinoyltrifluorborate anion was optimized because its presence is expected in solution. Reasonable correlations were observed between the predicted FTIR, Raman and UV−visible spectra with the corresponding experimental ones. The solvation energies for the salt in aqueous solution were predicted by using both methods. Here, it is observed that the change of furane by pyridine ring generates an increase in the solvation energies of the potassium 2-isonicotinoyltrifluorborate salt in relation to potassium 3-furoyltrifluoroborate salt. The study of the charges has revealed that there is an effect of the size of the basis set on the Mulliken charges while the AIM analyses suggest that the F···H and O···K interactions are also strongly dependent of the medium and the size of the basis sets. The bond orders for the F and K atoms evidence their higher ionic characteristics in solution with both basis sets. The NBO and AIM results clearly support the higher stability of this salt in both media. The studies by using the frontier orbitals indicate that the change of furane by pyridine ring decreases the reactivity of this salt by using 6-31G* basis set but increases when the other one is employed. Another effect of change of furane by pyridine ring is observed in the increase of the *f(νC═O)* and *f(νBF$_3$)* force constants. In addition, the force fields for the salt in both media were reported together to their complete vibrational assignments and force constants by using both levels of theory.

1. Introduction

The presence of different groups in the structure of the potassium 2-isonicotinoyltrifluoroborate salt confers interesting properties to this salt, hence, it can be used in organic synthesis chemistry especially in the acquisition of conjugated molecules, such as protein-proteins and protein-polymer [1–7]. In a recent study on the potassium 3-furoyltrifluoroborate salt by using the B3LYP/6-31G* and 6-311++G** methods the most stable structures of this salt have been optimized with C_s symmetries. The observed coordination numbers for the B and K atoms in those structures by using both levels of theory were five and four, respectively [8]. The presence of the furyl ligand in that salt linked to that (C═O)−BF_3K group notably reduces the gap value of furane ring in gas phase from 6.6434 eV to 4.5303 eV by using the B3LYP/6-31G* method while in aqueous solution its value is reduced from 6.6151 eV to 4.9546 eV increasing the reactivity of this salt in both media. On the other hand, the reactivity of this salt decreases in aqueous solution from 4.5303 eV in gas phase to 4.9546 eV in aqueous solution by using the same method [8]. Thus, the coordination modes of those (C═O)−BF_3K groups together with the ligand type to which the group is linked are important factors related to the stereochemistry of these salts. Evidently, there are structural and conformational

* Corresponding author.
E-mail address: sbrandan@fbqf.unt.edu.ar (S.A. Brandán).

https://doi.org/10.1016/j.molstruc.2018.02.098
0022-2860/

factors that have an influence on their reactivities, as reported in the literature [1–4,7]. Hence, the aim of this work is to study the structural and vibrational properties of the potassium 2-isonicotinoyltrifluoroborate salt because so far, those properties have not been reported and, only the synthesis of this salt and their characterization by NMR and mass spectroscopies were reported [3]. Therefore, it is necessary to know all the structural, electronic and topological properties related to that salt when the pyridine ring is linked to the (C═O)−BF_3K group in order to compare it to those properties reported for the potassium 3-furoyltrifluoroborate salt [8]. With these purposes, the potassium 2-isonicotinoyltrifluoroborate salt was first modeled and later optimized by using theoretical calculations derived from the density functional theory (DFT) with the hybrid B3LYP method and the two 6-31G* and 6-311++G** levels of theory in gas phase and in aqueous solution [9,10]. In solution, the interactions and the solvent effects were considered by using the integral equation formalism variant polarised continuum method (IEFPCM) [11,12] and the solvation model [13] in order to compute the solvation energies with both levels of theory. These calculations were combined with the experimental infrared and Raman spectra in order to perform the complete vibrational analysis by using the SQMFF methodology [14] and the Molvib program [15]. Here, we have studied the atomic Mulliken and natural population charges, the bond orders, the donor-acceptor energy interactions, the topological properties in both media by using the NBO and AIM calculations [16,17]. Additionally, the harmonic force constants and the frontier orbitals [18,19] were also calculated in order to predict the characteristics of all bonds and the reactivities and behavior of this salt in the two studied media. Here, the results obtained for this salt were then compared with those obtained for the potassium 3-furoyltrifluoroborate salt [8] in order to observe the changes in their properties when the furane ring is replaced by the pyridine one.

2. Experimental

A pure sample of potassium 2-isonicotinoyltrifluoroborate salt (ITFB) in the solid phase was used to record the infrared spectrum in KBr pellets in the 4000 to 400 cm^{-1} range by using a Perkin Elmer Spectrum GX spectrometer. The corresponding Raman spectrum was recorded in solid state at room temperature between 3600 and 100 cm^{-1} with the optical module of the Perkin Elmer Spectrum GX Raman equipped with an yttrium aluminum garnet crystal doped with triply-ionized neodymium laser (excitation line of 1064 nm, 1900 mW of laser power). The Raman spectrum was recorded with 100 scans and a resolution of 4 cm^{-1}. On the other side, a Beckman spectrophotometer was used to record the ultraviolet spectrum of ITFB in aqueous solution between 200 and 800 nm.

3. Computational details

Here, the *GaussView* program was used to build the initial structure of ITFB [20]. Then, this structure was optimized in gas phase and in aqueous solution by using the hybrid B3LYP/6-31G* and B3LYP/6-311++G** methods [9,10] with the Gaussian 09 program [21]. In solution, the IEFPCM model [11,12] was employed, as mentioned above. After that, the potential energy surfaces (PES) by using both levels of theory were studied modifying the dihedral C4−C5−C11−B13, C4−C5−C11−O12, N6−C5−C11−B13, N6−C5−C11−K17 and N6−C5−C11−O12 angles in those optimized structures. Thus, four stable structures were found on PES named C1, C2, C3 and C4, which can be seen in Fig. 1 and, where C4 is clearly the most stable conformation with minimum energy and higher populations in both media. C1 and C2 present C_1 symmetries while the symmetries predicted for C3 and C4 are C_S. Fig. 2 shows the C4 structure together with the atoms labeling. The high instabilities of C1, C2 and C3 are probably justified by the strong repulsions predicted between the lone pairs corresponding to the two electronegative F15 and N6 atoms while the distance between the N6 and O12 atoms predicted lower repulsions in C4. Obviously, only for C4 the atomic Mulliken were computed together with the natural population charges, molecular electrostatic potentials, bond orders, donor-acceptor energy interactions and the topological properties by using both levels of theory and the NBO and AIM2000 programs [16,17]. The C4 structure in aqueous solution was optimized by using the PCM/SMD models [11–13] with the Gaussian 09 program [21]. The vibrational analyses in both media were performed taking into account the normal internal coordinates and the harmonic force fields calculated with both methods by using the SQMFF procedure [14] and the Molvib program [15]. The normal internal coordinates for the BF_3 group belong to the BF_3K system and were built using C_{3v} symmetry and in accordance with the potassium 3-furoyltrifluoroborate salt [8] and to compounds containing CH_3 groups [22–24]. Here, the C4 structure in solution was also optimized with C_s symmetry, as was also observed in the potassium 3-furoyltrifluoroborate salt [8]. To perform the complete assignments of the bands observed in the infrared and Raman spectra to the vibration normal modes only those potential energy distribution (PED) contributions $\geq$ 10% were considered. The structures of two different dimeric species of C4 (Fig. 3) were also optimized in accordance with the layered architectures suggested for trifluoroborate potassium salts in the solid state by Kamiński et al. [25] and for other trifluoroborate salts recently reported [26,27]. The presence of both dimeric species is justified because there are better and reasonable concordances among their predicted vibrational spectra with the experimental ones and with that predicted for the monomer. Here, it is observed that some bands observed in the experimental Raman spectrum in the lower wavenumbers region clearly justify the presence of these two dimers. The experimental electronic spectrum of ITFB was recorded in aqueous solution and their corresponding theoretical spectrum was predicted in the same medium by using the Time-dependent DFT calculations (TD-DFT) with those two levels of theory and the Gaussian 09 program [21]. Here, the anion structure was also optimized in solution by using the B3LYP/6-311++G** method because its presence is expected in this medium. The PES for the anion shows two structures with the same energies and, for this reason, only one of them is presented in Fig. 4. After that, the experimental ultraviolet spectrum recorded for the salt was compared with that which predicted for the anion. In this case, as in the potassium 3-furoyltrifluoroborate salt [8], the frontier orbitals [18,19] were also calculated for C4 in both media together with the chemical potential (μ), electronegativity (χ), global hardness (η), global softness (S), global electrophilicity index (ω) and nucleophilicity indexes (E) descriptors [8,28,29] to predict their reactivities and behavior in the two media. In this way, the properties of those two potassium salts were compared with each other to know the effect of the pyridine ring on the (C═O)−BF_3K group. In particular, the nucleophilicity index was later compared with those similar parameters reported for reactions of organoboron compounds [30].

4. Results and discussion

4.1. Geometries in gas and in aqueous solution phases

For C4 of ITFB in both media, the total and relative energies, dipolar moments, volume variations, populations and, the different

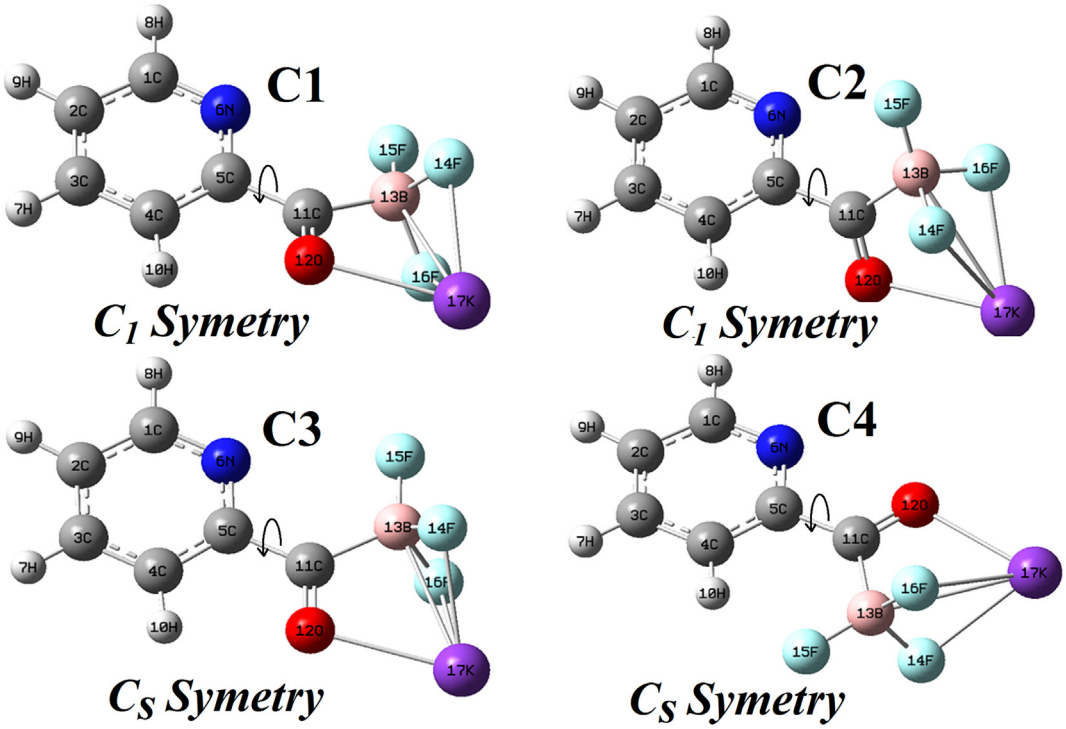

Fig. 1. Molecular structures of the more stable conformers for the potassium 2-isonicotinoyltrifluorborate salt and their corresponding symmetries. With τ letter is indicated the different dihedral N6–C5–C11–B13 angle.

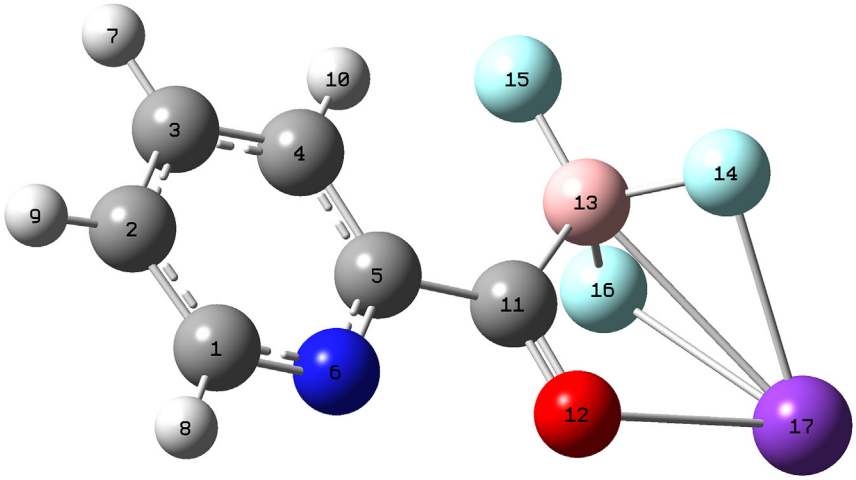

Fig. 2. Molecular structure of the most stable C4 conformer for the potassium 2-isonicotinoyltrifluorborate salt and atoms numbering.

dihedral angles studied by using the B3LYP/6-31G* and B3LYP/6-311++G** methods, are presented in Table 1. The volume values in gas phase for the four conformers and their variations in solution were computed from the differences between the values obtained in solution and in gas phase by using the Moldraw program [31]. Regarding the relative energy values we can observe that only C4 is the most stable structure in both media with minima energies and higher populations. Note that C4 structures present higher expansion volumes in solution in relation to the other ones. Besides, C1 and C2 in both media have the same energies and C_1 symmetries, low populations but opposite dihedral angles, as observed in Table 1. For these reasons, only the properties for C4 are presented in this study. Here, C4 was optimized in both media with C_S symmetries, as in the potassium 3-furoyltrifluoroborate salt [8]. C4 shows lower dipole moment values in both media with the direction of their vector oriented from the F atoms toward the K atom, as in the furyl salt [8] and as observed for this salt in gas phase in Fig. S1. The predicted dipole moment value corresponding to the anion in solution is 14.93 D by using the B3LYP/6-311++G** level of theory while the salt in solution presents a dipole moment value of 5.40 D. Evidently, the presence of K^+ cations notably reduces their value in solution. The predicted solvation energy value for ITFB by using the 6-31G* and 6-311++G** basis sets are presented in Table 2 and, their values are respectively −82.68 and −90.65 kJ/mol different from those obtained for the potassium 3-furoyltrifluoroborate salt [8] of −75.79 and −81.55 kJ/mol, respectively. Here, although the furoyl salt has higher dipole moment and volume values in both media, it has lower solvation energy values

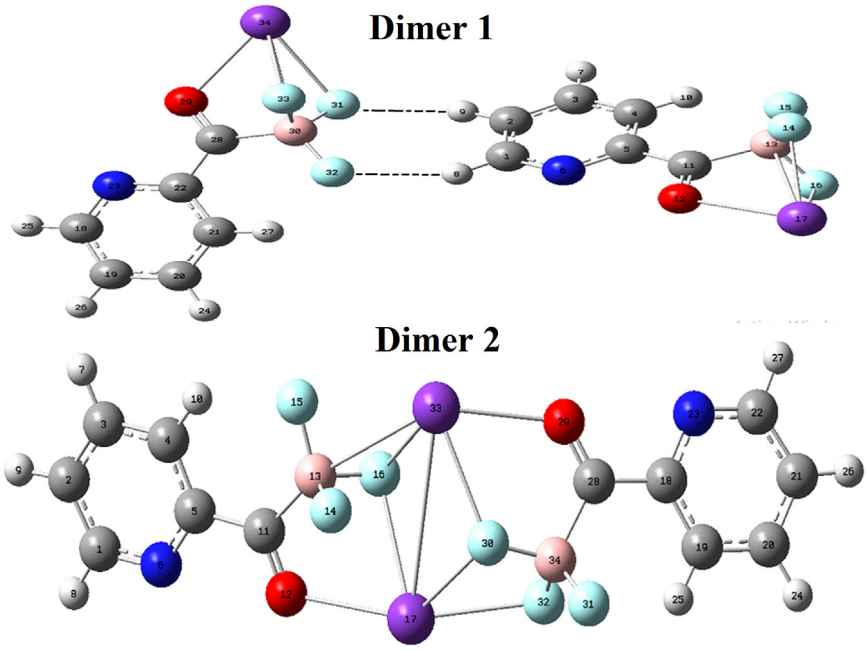

Fig. 3. Theoretical molecular structures of two dimeric species of 6-Potassium 2-isonicotinolfluoborate salt according to X-ray structure from: a) Ref. [27] dimer 1 and b) Ref. [25] dimer 2 together with the atoms numbering. Intramolecular H-bonds are represented with dashed lines.

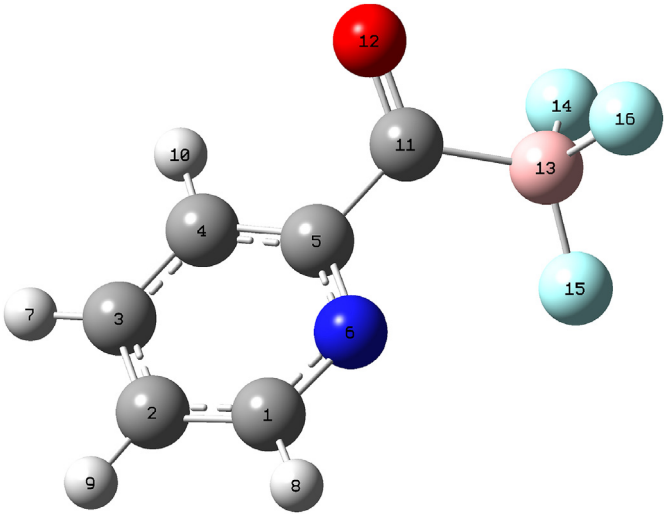

Fig. 4. Theoretical molecular structure of 2-isonicotinolfluoborate anion and the atoms numbering.

than ITFB. In that salt, probably the influence of the furyl ring on their properties could be justified by the formation of two H bonds that generate lower solvation in solution, as compared with ITFB. When the solvation energy value for C4 of ITFB is compared with that reported for the picosulphate salt [32], we observed that there are higher differences between these two salts because the solvation energy value in picosulphate is −254.38 kJ/mol while their volume variation is 13.3 $Å^3$. Obviously, the high dipole moment value of 15.14 D observed for picosulphate in solution could explain in part the differences with the isonicotinoyl salt.

Table 3 shows the calculated geometrical parameters for C4 of ITFB compared with the experimental ones obtained for crystal structures of pyridine and pyridine trihydrate [33], for potassium trifluoro[(*Z*)-3-methoxyprop-1-enyl]borate [34] and for potassium trifluoro[(*Z*)-3-(oxan-2-yloxy)prop-1-en-1-yl] borate monohydrate [35] by using the root-mean-square deviation (RMSD) values. The structures of these compared compounds can be seen in Fig. S2 while in Fig. S3 the two potassium salts, 3-furoyltrifluoroborate [8] and 2-isonicotinoyltrifluoroborate are presented. The most stable C4 structure for ITFB was also optimized with C_s symmetry, as in the potassium 3-furoyltrifluoroborate salt [8] by using the two levels of calculations. Evidently, in both salts there are structurals preferences of the trifluoroborate group for that symmetry. In ITFB, as in the furoyltrifluoroborate salt, the B and K atoms are in the same plane of the rings, in this case the pyridine rings, and where those two atoms have coordinations number five and four, respectively as observed in Fig. 2. In Fig. S2 we can see the common part of those structures [33–35] which were compared with ITFB. In general, we can clearly observe correlations for bond lengths between 0.205 and 0.020 Å while for bond angles between 4.1 and 1.9°; where our parameters bond lengths are better correlated with the potassium trifluoro[(*Z*)-3-(oxan-2-yloxy)prop-1-en-1-yl] borate monohydrate [35] salt while for the bond angles the better correlations can be observed for pyridine and pyridine trihydrate [33]. In relation to the dihedral angles, the calculated values for ITFB were compared with those reported for the furoyltrifluoroborate salt [8] in gas and aqueous solution phases by using the B3LYP/6-311++G** method. The results show high RMSD values (146.9–146.8°) which indicate clear differences between the dihedral angles of both ITFB and 3-furoyltrifluoroborate salts due to the different pyridine and furane rings, respectively present in their structures.

4.2. Charges, MEP and bond orders studies

In this salt, as in the furoyl salt [8], different interactions are expected in ITFB due to the presence of the pyridine ring and to the two electronegative atoms present in the (C═O)–BF_3K group. Hence, it is very important to investigate the nature of these interactions and, for these reasons, the Mulliken and atomic natural population charges were computed by using both methods and in

Table 1
Calculated total (E) and relative energies (ΔE), dipole moments (μ), molecular volume (V) and volume variations (ΔV) and populations (%) for the Potassium 2-isonicotinoyltrifluorborate salt. The studied diehedral angles are also included.

GAS PHASE/B3LYP/6-31G*method											
Conformers	E (Hartrees)	μ (Debye)	V (Å^3)	ΔE (KJ/mol)	ΔV (Å^3)	Population (%)	Dihedral angles (°)				
							N6C5C11B13	N6C5C11K17	N6C5C11O12	N6C5C11O12	N6C5C11O12
C1	−1285.5401	7.9696	236.8	8.13		3.34	−9.6	157.5	170.3	−9.3	170.6
C2	−1285.5401	7.9703	241.2	8.13		3.34	9.6	−157.5	−170.3	9.3	−170.6
C3	−1285.5400	7.9754	242.3	8.39		3.07	0.0	180.0	180.0	0.0	180.0
C4	−1285.5432	5.6534	240.1	0.00		90.25	180.0	0.0	0.0	180.0	0.0
AQUEOUS SOLUTION/PCM/B3LYP/6-31G*method											
C1	−1285.5671	9.6180	236.9	9.18	0.1	2.26	−16.5	118.8	161.5	−17.3	164.5
C2	−1285.5670	7.8665	242.1	9.44	1.0	2.27	16.5	−118.8	−161.5	19.2	−162.6
C3	−1285.5670	9.7146	244.1	9.44	1.8	2.27	0.0	180.0	180.0	0.0	180.0
C4	−1285.5706	5.5218	243.0	0.00	2.9	93.17	180.0	0.0	0.0	180.0	0.0
GAS PHASE/B3LYP/6-311++G**method											
Conformers	E (Hartrees)	μ (Debye)	V (Å^3)	ΔE (KJ/mol)	ΔV (Å^3)	Population (%)	Dihedral angles (°)				
							N6C5C11B13	N6C5C11K17	N6C5C11O12	N6C5C11O12	N6C5C11O12
C1	−1285.7901	8.1245	241.1	6.30		6.78	23.1	−129.1	−156.7	22.3	−157.6
C2	−1285.7901	8.1282	240.6	6.30		6.78	23.2	−128.4	−156.6	22.4	−157.6
C3	−1285.5899	8.5487	243.9	31.41		0.00	0.0	180.0	180.0	0.0	180.0
C4	−1285.7925	5.5569	220.3	0.00		86.44	180.0	0.0	0.0	180.0	0.0
AQUEOUS SOLUTION/PCM/B3LYP/6-311++G**method											
C1	−1285.8202	10.2769	232.6	7.34	−8.5	4.67	27.1	−107.4	−151.5	27.0	−154.1
C2	−1285.8202	10.2803	236.5	7.34	−4.1	4.67	27.2	−107.4	−151.5	27.0	−154.1
C3	−1285.8117	10.5913	244.5	29.63	0.6	0.00	0.0	180.0	180.0	0.0	180.0
C4	−1285.8230	5.4016	242.9	0.00	22.6	90.66	180.0	0.0	0.0	180.0	0.0

Table 2
Calculated solvation energies (ΔG) for the most stable C4 conformer of the Potassium 2-isonicoinoyltrifluoroborate salt by using the B3LYP/6-31G* and B3LYP/6-311++G** methods.

Solvation energies (kJ/mol)			
Method	$\Delta G_u^{\#}$	ΔG_{ne}	ΔG_c
B3LYP/6-31G*	−68.77	13.91	−82.68
B3LYP/6-311++G**	−76.55	14.09	−90.65

$\Delta G_u^{\#}$ = Uncorrected values; ΔG_{ne} = Non electrostática terms; ΔG_c = Corrected values.

the two studied media. In Table S1 the comparisons of the two charges are presented by using both methods while in Fig. S4 the values in gas phase and in aqueous solution with the two methods are presented. The graphics for both charges by using the B3LYP/6-31G* level show the same behavior in both media and where the NPA charges present higher values than the Mulliken ones. Besides, the NPA charges predicted higher values on the B13 atoms than the K17 ones while; on the contrary, the Mulliken charges predicted higher values on the K17 atoms in both media. On the other hand, both charges show the same behavior in the two studied media and with the two basis sets. Higher modifications are observed when the Mulliken charges values on all atoms by using the 6-311++G** basis set are compared with those observed with the 6-31G* basis set. Hence, the Mulliken charges on the C4 and H9 atoms notably increase their values while the charge on the H7 atoms are more negative together with the charges on the H10 and O12 atoms. These facts can be easily explained due to the H bonds formed between the F15 and H10 atoms, as we will see later in the NBO analysis in both media. This way, Fig. S5 shows clearly that the Mulliken charges are strongly affected by the size of the basis set.

Taking into account the great difference between the values of both charges, for ITFB we have studied the molecular electrostatic potential mapped (MEP) because these surfaces are very interesting to investigate the nucleophilic and electrophilic sites where different regions take place. Thus, these regions for ITFB in gas phase by using the B3LYP/6-31G* method are given in Fig. S6. Here, the slight red colours are observed on the N6, O12 and F14, F15 and F16 atoms indicating clearly that these regions are nucleophilic sites while a strong blue color is only observed on the K atom which indicates that it is an electrophilic region. A very important detail is also observed in the potassium 3-furoyltrifluoroborate salt in gas phase: the color ranges predicted for the mapped surface by using the B3LYP/6-31G* method are the same for both salts (From red −0.116 to blue +0.116 au). Hence, the reaction sites are obviously predicted by this MEP with probably a higher electrophilic character, as revealed by their mapped surface.

For ITFB in both media and with the two basis sets, the bond orders (BO) were computed and expressed as Wiberg indexes because the nature of the different bonds can be easily analyzed with these parameters if the characteristics of these bonds are considered. These results are presented in Table S2 while the graphics of their variations in gas and solution phases by using the two basis sets can be seen in Fig. S7. First, we observed that both graphics have the same behavior in both media where the higher values are observed in the C atoms that belong to the pyridine rings (From C1 to C5), as it was expected because these atoms have double bond characters and where the low BO values are observed for the H atoms and, especially in the F and K atoms because these atoms show strong ionic bonds, as revealed by the Matrix bonds orders presented in Table S2. Note that in solution with both basis sets the BO values for the F and K atoms decrease because it is clear that these atoms show their higher ionic characteristics in this medium.

4.3. NBO and AIM study

The studies above have shown the strong ionic character of this ITFB salt, especially in solution and, for these reasons; their

Table 3
Comparison of calculated geometrical parameters for the Potassium 2-isonicoinoyltrifluoroborate salt in both media by using two levels of theory.

B3LYP method[a]					Experimental		
Parameters	6-31G*		6-311++G**		EXP[b]	EXP[c]	EXP[d]
	Gas	PCM	Gas	PCM			
Bond lengths (Å)							
C1–C2	1.401	1.400	1.399	1.398	1.368		
C2–C3	1.390	1.389	1.387	1.386	1.370		
C3–C4	1.395	1.396	1.394	1.394	1.375		
C4–C5	1.402	1.399	1.399	1.396	1.375		
C5–N6	1.349	1.353	1.345	1.350	1.344		
N6–C1	1.330	1.333	1.327	1.330	1.333		
C1–H8	1.089	1.088	1.087	1.085	0.920		
C2–H9	1.086	1.085	1.083	1.083	0.950		
C3–H7	1.086	1.085	1.084	1.083	0.930		
C4–H10	1.082	1.081	1.080	1.079	1.030		
C5–C11	1.509	1.503	1.509	1.501			
C11═O12	1.242	1.249	1.235	1.239			
C11–B13	1.660	1.652	1.659	1.651		1.615	1.582
B13–F14	1.437	1.429	1.447	1.439		1.420	1.426
B13–F15	1.380	1.393	1.383	1.399		1.415	1.392
B13–F16	1.437	1.429	1.447	1.439		1.440	1.439
K17–B13	2.951	3.053	2.990			3.405	
K17–F14	2.555	2.648	2.583	2.708			
K17–F16	2.555	2.648	2.583	2.708			
K17–O12	2.588	2.692	2.54	2.699			
RMSD[b]	**0.089**	**0.087**	**0.086**	**0.085**			
RMSD[c]	**0.205**	**0.159**	**0.188**	**0.020**			
RMSD[d]	**0.040**	**0.035**	**0.040**	**0.035**			
Bond angles (°)							
C1–C2–C3	118.2	118.3	118.2	118.3	118.7		
C2–C3–C4	118.7	118.5	118.7	118.6	118.3		
C3–C4–C5	118.8	119.1	118.8	119.1	119.0		
C5–N6–C1	117.7	117.6	118.0	117.9	115.9		
N6–C1–C2	123.8	123.8	123.6	123.6	124.1		
N6–C1–H8	116.1	116.3	116.2	116.4	116.0		
C2–C1–H8	120.0	119.7	120.0	119.9	115.0		
C1–C2–H9	120.2	120.1	120.2	119.8	120.0		
C3–C2–H9	121.5	121.5	121.5	121.5	120.0		
C2–C3–H7	120.8	120.9	120.8	120.9	117.0		
C4–C3–H7	120.4	120.4	120.3	120.3	120.0		
C3–C4–H10	121.6	120.9	121.3	120.5	121.0		
C5–C4–H10	119.4	119.8	119.8	120.2	119.0		
C4–C5–N6	122.5	122.3	122.3	122.2	124.1		
C5–N6–C1	117.7	117.6	118.0	117.9	115.9		
C5–C11═O12	117.5	117.9	118.1	118.8			
C5–C11–B13	126.2	126.6	126.2	126.7			
C11–B13–F14	105.8	106.4	106.0	106.8		110.7	109.4
C11–B13–F15	117.5	117.6	118.4	118.8		114.6	116.4
C11–B13–F16	105.8	106.4	106.0	106.8		111.1	113.2
C11═O12–K17	108.2	109.8	110.1	112.5			
F14–B13–F15	110.4	109.5	110.2	108.9		105.9	106.2
F14–B13–F16	105.7	106.5	104.6	105.6		105.8	103.5
F15–B13–F16	110.4	109.5	110.2	105.6		108.1	107.2
F14–K17–F16	53.2	51.1	52.6	50.0			
F14–K17–O12	67.6	64.6	67.0	63.5			
F14–K17–B13	29.1	27.9	28.9				
B13–K17–O12	52.5	50.1	51.7	48.9			
F16–K17–O12	67.6	64.6	67.0	63.5			
F16–K17–B13	29.1	27.9	28.9				
RMSD[b]	**1.9**	**1.8**	**1.9**	**1.9**			
RMSD[c]	**3.8**	**3.3**	**3.8**	**3.3**			
RMSD[d]	**4.1**	**3.7**	**3.9**	**3.4**			
Dihedral angles (°)							
C5–C11–B13–F14	124.0	123.2	124.5	123.6	124,2[e]	123,2[f]	
C5–C11–B13–F15	0.0	0.0	0.0	0.0	−0,04[e]	−0,04[f]	
C5–C11–B13–F16	−124.0	−123.2	−124.5	−123.6	−122,9[e]	−123,3[f]	
O12–C11–B13–F14	−55.9	−56.7	−55.4	−56.3	−55,8[e]	−56,7[f]	
O12–C11–B13–F15	−180.0	−180.0	−180.0	−180.0	179,9[e]	179,9[f]	
O12–C11–B13–F16	55.9	56.7	55.4	56.3	55,7[e]	56,6[f]	
N6–C5–C11–B13	180.0	180.0	180.0	180.0			

Table 3 (*continued*)

B3LYP method[a]					Experimental		
Parameters	6-31G*		6-311++G**		EXP[b]	EXP[c]	EXP[d]
	Gas	PCM	Gas	PCM			
RMSD[e]	**146.9**	**146.9**	**146.9**	**146.9**			
RMSD[f]	**146.8**	**146.8**	**146.8**	**146.9**			

[a] This work.
[b] From Ref [33].
[c] From Ref [34].
[d] From Ref [35].
[e] B3LYP/6-311++G** in gas phase from Ref. [8].
[f] B3LYP/6-311++G** in aqueous solution from Ref. [8].

stabilities should be examined by using NBO and AIM calculations [16,17]. The study of the donor-acceptor energy interactions in gas phase and in aqueous solution by using both basis sets are summarized in Table S3. Exhaustively considering the results, we observed that a higher number of transitions are observed in this ITFB salt in relation to the potassium 3-furoyltrifluoroborate salt [8], thus, the $\Delta E_{\pi\rightarrow\pi^*}$, $\Delta E_{n\rightarrow\sigma^*}$, $\Delta E_{\pi^*\rightarrow\pi^*}$, $\Delta E_{\pi^*\rightarrow n^*}$, $\Delta E_{n\rightarrow n^*}$ and $\Delta E_{n^*\rightarrow n^*}$ interactions are observed with both basis sets but the $\Delta E_{\pi^*\rightarrow n^*}$ interactions are only observed for the salt in both media using the 6-31G* basis set while the *LP(2)O12→ σ*C11−B13* transition is only observed for the salt in solution and with the 6-311++G** basis set. Note that the most important interactions are the $\Delta E_{n\rightarrow n^*}$ interactions, those observed from the lone pairs of the F atoms towards the B atoms with higher total contributions to the total energies for the salt being observed in both media and with the 6-311++G** basis set. These results clearly evidence that this salt exhibits higher stability than the potassium 3-furoyltrifluoroborate salt [8].

In accordance with the Bader's theory the topological properties are indispensable parameters to examine the different intramolecular interactions that are present in a molecule [36]. Thus, the AIM2000 program [17] was employed to compute the electron density distribution, $\rho(r)$ and the Laplacian values, $\nabla^2\rho(r)$, the eigenvalues $(\lambda1, \lambda2, \lambda3)$ of the Hessian matrix and the $\lambda1/\lambda3$ ratio in the bond critical points (BCPs) and, in the ring critical points (RCPs). These results are presented in Table S4 for ITFB in both media and by using the two basis sets. Regarding these values we observed that $\lambda1/\lambda3 < 1$ and $\nabla^2\rho(r) > 0$ in the BCPs for which is predicted an intra-molecular H bond and three ionic interactions which are respectively, F15···H10, F14−K17, F16−K17 and K17−O12, having this latter interaction high densities with both basis sets, as observed in the furoyl salt [8]. These interactions are designed as closed-shell and all the details for ITFB in gas phase by using 6-31G* basis set can be seen in the molecular model presented in Fig. 5. Here, as in the potassium 3-furoyltrifluoroborate salt [8], the pyridine ring is named RCP while RCPN1, RCPN2, RCPN3 and RCPN4 are the new RCPs formed, as shown in Fig. 3. A very important result in this salt, different from the furoyl salt [8], is that in ITFB in both media and with the two basis sets the same interactions are observed while in the furoyltrifluoroborate salt [8] in gas phase the number of interactions decreases by using the 6-311++G** basis set increasing the parameters values. Calculated topological parameters corresponding to the F16···K17 and F14···K17 ionics, O12···K17 and F15···H10 bonds interactions for the salt in both media and by using the two levels of theory can be seen in Fig. S8. This Figure clearly shows that the two ionic interactions have different properties in both media and by using the two basis sets while the other two F15···H10 and O12···K17 interactions have some common properties. Thus, in the F15···H10 interaction the $\lambda3$ and $|\lambda1/\lambda3|$ parameters present practically the same values in both media but their properties slightly change when the other basis set is used. However, in the O12···K17 interaction all properties in gas phase present the same values independently from the basis set while the values change in solution by using the two basis sets.

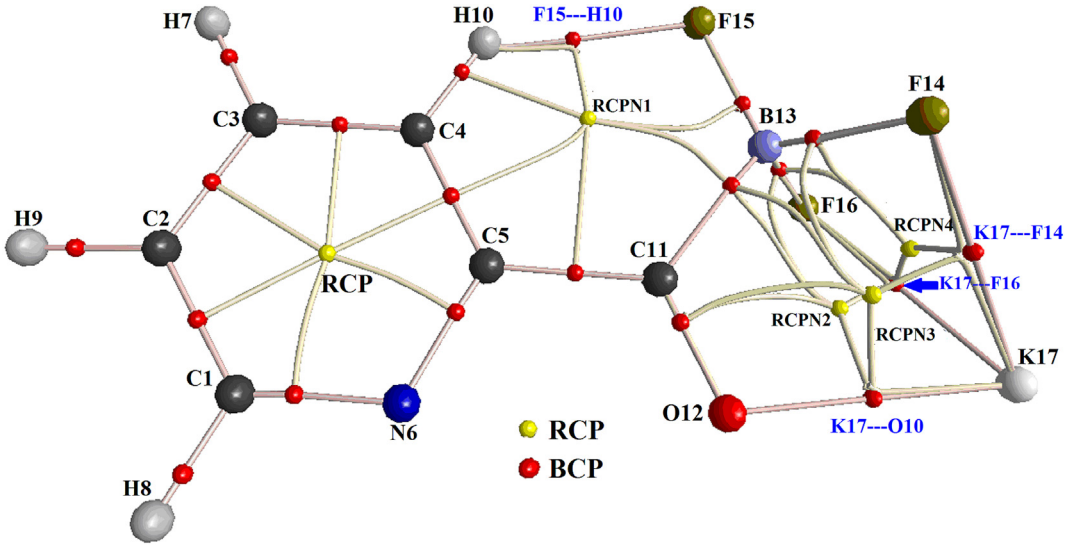

Fig. 5. Molecular graphics for the potassium 2-isonicotinoyltrifluorborate salt in gas phase showing the geometry of all their bond critical points (BCPs) and ring critical points (RCPs) at the B3LYP/6-311++G** level of theory.

Here, the pyridine ring in both media and by using the two basis sets presents higher topological parameters in relation to the other ones, as expected because it belongs to ITFB.

The study performed for ITFB by using NBO calculations clearly supports the high stabilities of this salt in the two different media, as revealed by the elevated energy values predicted in gas phase and in solution (7063.90 and 6760.50 kJ/mol by using 6-31G* and 6-311++G** basis sets, respectively and of 7753.24 and 7089.48 kJ/mol by using 6-31G* and 6-311++G** basis sets, respectively). On the other hand, the four interactions predicted for ITFB in both media by using AIM analysis also evidence the high stability of this salt as a consequence of those four different interactions observed.

4.4. Frontier orbitals and global descriptors

Here, the gap values were calculated by using the frontier orbitals [18,19], as suggested by the literature, and with these values the global parameters were computed, such as chemical potential (χ), electronegativity (μ), hardness (η), softness (S), electrophilicity index (ω) and nucleophilicity index (E) [8,22–24,28–30]. Table S5 shows the values for potassium 2-isonicotinolfluoborate compared with those obtained for the potassium 3-furoyltrifluoroborate salt [8]. When the gap values are compared by using the two basis sets we observed that the reactivities of IFTB in gas phase decrease in solution with the 6-31G* basis set but by using 6-311++G** basis set their value slightly increases in solution. These results are different from those observed for the potassium 3-furoyltrifluoroborate salt [8]. In relation to the descriptors, both basis sets show higher electrophilicity indexes in the pyridine salt than the furyl salt in the two media while higher nucleophilicity indexes are observed in the furyl salt than the pyridine one. The nucleophilicity index obtained for this salt in water (8.71 eV) coincides with that obtained of 7.66 eV for benzhydrylium salt in acetonitrile by Berionni et al. [30]. Probably, the presence of the C=O group linked to the ring in this salt differs from the benzhydrylium one, justifying the difference observed. These studies show that IFTB is less reactive in solution by using the 6-31G* basis set, as the potassium 3-furoyltrifluoroborate salt [8]. Hence, the decrease in the reactivity of this IFTB salt in solution could probably be justified by the diminishing of the total delocalization energies in solution, in relation to the values in gas phase, observed by the NBO analysis with both basis sets.

4.5. Vibrational analysis

The potassium potassium 2-isonicotinoyltrifluoroborate salt was optimized with C_s symmetry in both media and by using the two basis sets, hence, 39 vibration normal modes actives in both IR and Raman spectra are expected for this salt. These modes are classified as, 26 A'+ 13 A'' where the A' modes are planar while the A'' modes are out-of-plane. The experimental IR and Raman spectra of ITFB are given in Figs. 6 and 7, respectively. Both spectra were compared with the respective predicted for monomer and dimers in gas phase by using the 6-311++G**. The correlations between experimental and theoretical spectra are reasonable taking into account that the experimental spectra were recorded in the solid state while the corresponding predicted were calculated in gas phase where the forces packing among the molecules were not considered and, besides, all the frequencies were calculated considering harmonics movements. On the other hand, the intense bands predicted in the IR spectrum of monomer at 1139 and 877 cm^{-1} in the experimental one are both observed with lower intensity. This observation can be easily justified by the dimer 1 because both bands have lower intensities while the patter of bands in the 1144-945 cm^{-1} region can be attributed to dimer 2. Hence, bands that are not attributed to the monomer can be easily justified by the presence of both dimers. When the scattering activities predicted in the Raman spectra were transformed to intensities, a better correlation between both experimental and theoretical spectra is observed in Fig. 7 [37]. Besides, when the predicted Raman spectra for both dimers are carefully compared with the experimental one in Fig. S9 we clearly observed two bands at 748 and 676 cm^{-1} and one band at 796 cm^{-1} that justifies the presence of both dimers. To calculate the harmonic force fields, the SQMFF methodology [14] was used together with the internal normal coordinates for the most stable C4 conformer of ITFB by using the Molvib program [15]. The complete assignments of the vibrational spectra of ITFB were performed by using the harmonic force fields with both methods and in the two media taking into consideration the potential energy distribution (PED) contributions $\geq$ 10%. Hence, in Table 4 the experimental and calculated wavenumbers are summarized together with the complete assignments for this salt in both media and by using the two methods. Here, the normal internal coordinates used for the trifluoroborate group and for the pyridine ring of ITFB were similar to those reported for molecules containing analogous groups [8,22–24,38–40]. Below, we have discussed the assignments of some groups.

4.5.1. Band assignments

4.5.1.1. CH modes. In the furoyltrifluoroborate salt [8] the three expected C–H stretching modes were assigned between 3161 and 3133 cm^{-1}. In this ITFB salt, four C–H stretching modes with A' symmetries are expected between 3144 and 3007 cm^{-1}, hence, these modes are assigned to the IR and Raman bands between 3132 and 3001 cm^{-1}, as detailed in Table 4. A very important difference to observe in this salt is that the in-plane deformation or rocking modes are predicted to higher wavenumbers in relation to the furoyl one [8]. Thus, in FTFB, the in-plane deformation or rocking modes and the corresponding out-of-phase modes that were assigned between 1238/1002 and 873/733 cm^{-1}, respectively while, for ITFB, these modes can be easily assigned to the groups of IR and Raman bands between 1567/1128 and 1002/673 cm^{-1}, respectively. Here, we observed that in ITFB salts some out-of-phase modes were predicted with A' symmetries, as also observed in FTFB [8].

4.5.1.2. BF_3 modes. For ITFB, as in the FTFB salt [8], the vibration modes corresponding to the BF_3 group are predicted in different regions and with different symmetries. Thus, the SQM/B3LYP/6-31G* calculations in solution predicted the three stretching modes with A' symmetry while by using the other basis set the calculations in the same medium predicted only an antisymmetric stretching mode with this symmetry. Therefore, the IR and Raman bands located at 1106/1126, 997, 986, 891/880 and 789 cm^{-1} are assigned to the antisymmetric and symmetric stretching modes that are expected for this group [29] and, where their corresponding symmetries can be easily observed from Table 4. From three expected antisymmetric and symmetric deformation modes the SQM/B3LYP/6-31G* calculations in both media and the SQM/B3LYP/6-311++G** calculations in solution predicted an antisymmetric and their corresponding symmetrical modes with A' symmetry while in gas phase by using the basis set of higher size only one of these modes is predicted with this symmetry while the other two ones with A'' symmetry. Hence, these modes are associated with the IR and Raman bands observed at 582, 528, 444, 432 and 418 cm^{-1}. In the FTFB salt [8] these modes were assigned to the bands at 617/598, 467/452 and 417/403 cm^{-1}. Regarding the BF_3 rocking modes, in the FTFB salt [8] were assigned to the Raman bands at 244/236 and 242/232 cm^{-1}. In this IFTB salt, these modes are assigned to the Raman bands at 249 and 223 cm^{-1}. The twisting

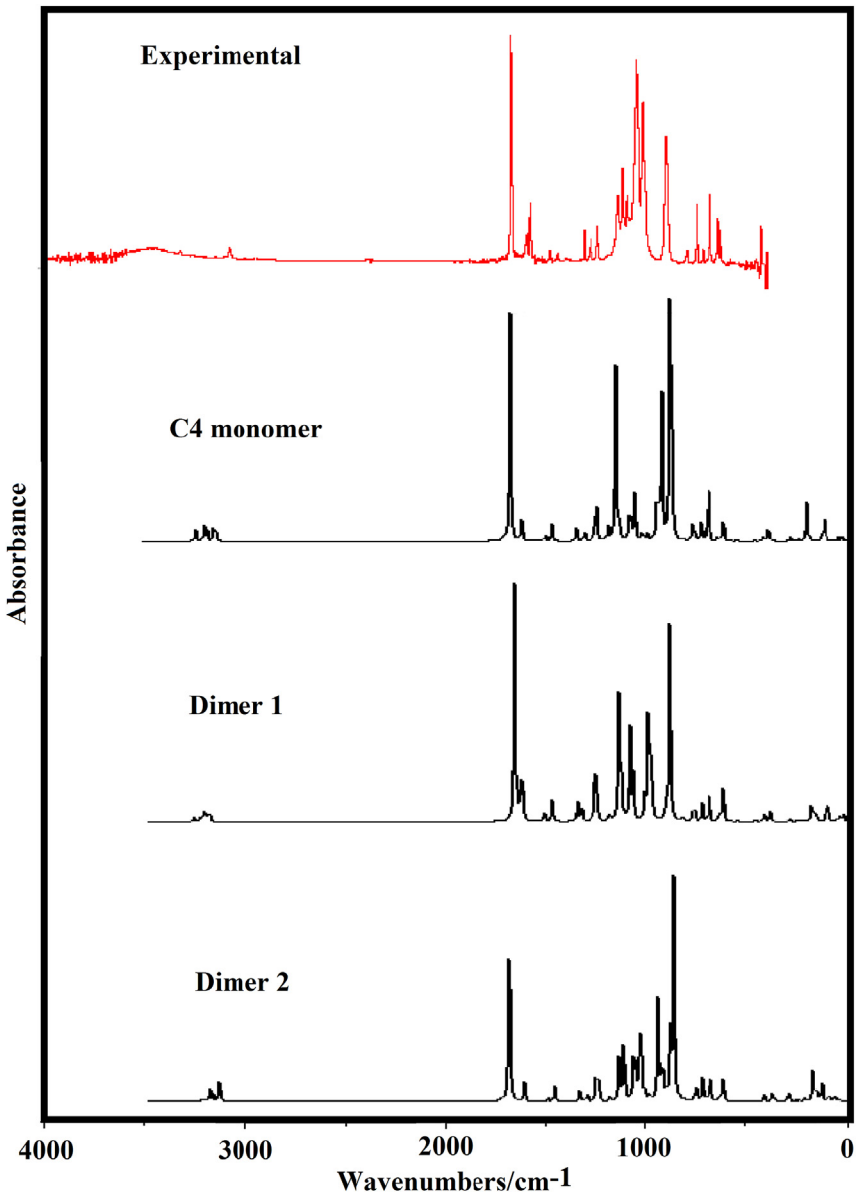

Fig. 6. Experimental infrared in the solid state of the potassium 2-isonicotinoyltrifluorborate salt compared with the corresponding predicted for the C4 conformer and their dimers by using B3LYP/6-311++G** level of theory.

modes in FTFB [8] were predicted with A″ symmetry between 37 and 21 cm^{-1} while in this salt they are predicted with the same symmetry between 169 and 144 cm-1. These modes in both salts were no assigned because the Raman spectrum was recorded from 4000 to 100 cm^{-1}.

4.5.1.3. Skeletal modes. In this salt, the C11═O12 stretching modes are predicted by SQM/B3LYP calculations with A′ symmetry and between 1621 and 1572 cm^{-1} [40] while in the furoyl salt [8] these modes were predicted between 1582 and 1556 cm^{-1}. Hence, in IFTB they are clearly assigned to the strong IR and Raman band at 1660 cm^{-1}. The C3═C4 stretching modes belong to the pyridine ring in both media and are predicted at higher wavenumbers than the other C1–C2, C2–C3 and C4–C5 stretching modes indicating, obviously, that they have different characteristics, thus, the strong Raman band at 1582 cm^{-1} is assigned to the C3═C4 stretching modes because they have double bonds character. The two expected C–N stretching modes belonging to the pyridine ring are predicted by the SQM calculations with different symmetries and in different regions [39]. Hence, the C1–N6 stretching are calculated with A′ symmetries at 1307/1290 cm^{-1} while the other C5–N6 stretching modes are predicted with A″ symmetries at 979/970 cm^{-1}. The exception in IFTB is observed for the C5–N6 stretching mode in solution by using the B3LYP/6-311++G** method because it presents A′ symmetry and it is predicted at 967 cm^{-1}, as indicated in Table 4. The C5–C11 stretching modes are predicted in different regions by using the B3LYP/6-31G* and B3LYP/6-311++G** methods and, also taking into account the media with different symmetries. Hence, with the first method in gas phase they are predicted at 448 (A″) cm^{-1} while in aqueous solution at 444 cm^{-1} (A′) cm^{-1}. With the basis set of higher size those modes are predicted in gas phase at 1144 cm^{-1} and, at 1153 cm^{-1} in aqueous solution. For these reasons, all C–N and C–C stretching modes are assigned in the predicted regions by the SQM calculations, as summarized in Table 4. In the furoyl salt [8], the two F–K stretching modes are predicted by using the 6-31G* and 6-

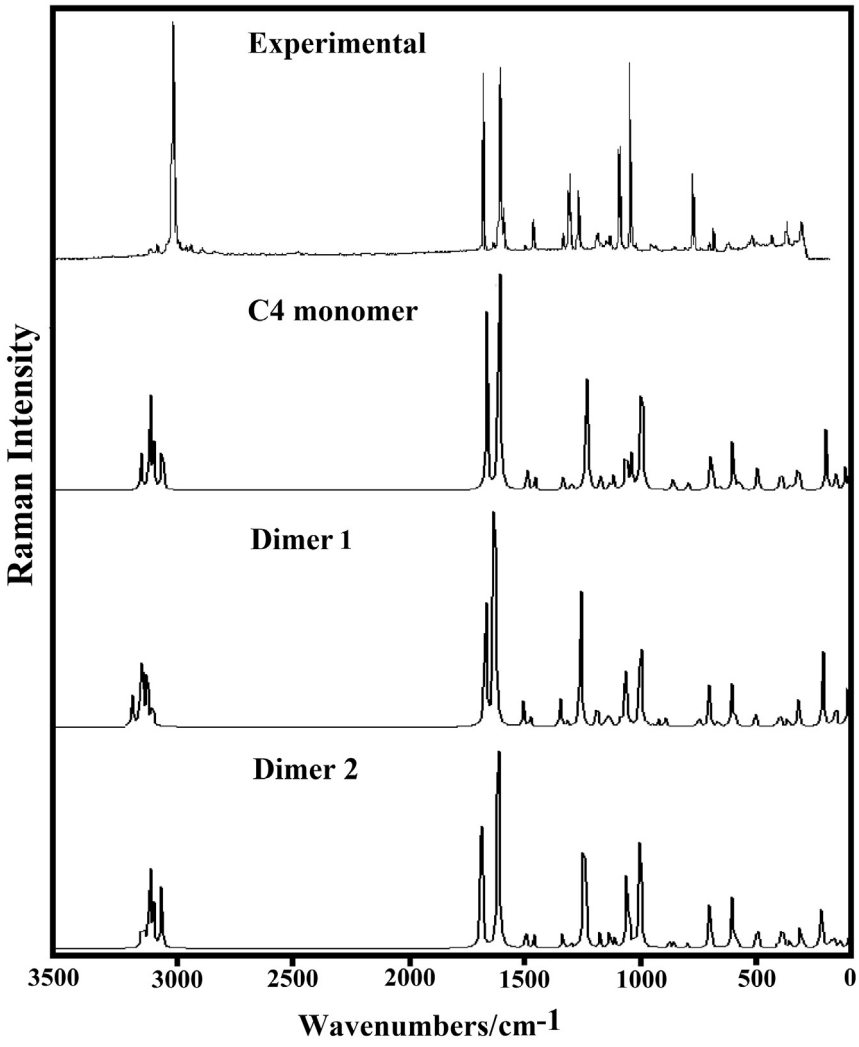

Fig. 7. Experimental Raman in the solid state of the potassium 2-isonicotinoyltrifluorborate salt compared with the corresponding predicted for the C4 conformer and their dimers by using B3LYP/6-311++G** level of theory.

311++G** basis sets with different symmetries and, for this reason; they were assigned to the Raman bands between 190 and 111 cm^{-1}. In this salt, when the 6-31G* basis set is employed the F16–K17 stretching modes are predicted with A′ symmetry in gas phase at 202 cm^{-1} while in solution at 171 cm^{-1}, hence, both modes were assigned to the Raman band at 193 cm^{-1}. The other F14–K17 stretching modes are predicted with A″ symmetry in gas phase at 127 cm^{-1} while in solution at 94 cm^{-1}, hence both modes were assigned to the Raman band at 123 cm^{-1}. With the other basis set some important differences are observed, because in gas phase the F16–K17 and F14–K17 stretching modes are predicted with symmetries A′ and A″ and at 189 and 113 cm^{-1}, respectively while in solution the F14–K17 and F16–K17 stretching modes are predicted at 143 and 69 cm^{-1}, respectively. Therefore, these modes are assigned in accordance with the SQM calculations. In relation to the three expected deformation ring modes (βR_1, βR_2, βR_3) for the salt in both media, the 6-31G* basis set predicted those modes with A′ symmetries at 1027/1024, 702/701 and 627 cm^{-1}. A same prediction can be seen for those three modes in gas phase by using the 6-311++G** basis set but, in solution two of these modes (βR_1, βR_3) are predicted with A′ symmetries and the remains βR_2, with A″ symmetry at 698 cm^{-1}. Hence, they were assigned accordingly [39]. On the other hand, two of the three torsion rings modes (τR_1, τR_2) are predicted in gas phase and with both basis sets with A″ symmetries at 735/733 and 416/413 cm^{-1} while in solution by using 6-31G* basis set the three modes are predicted with A″ symmetries. In solution and by using the 6-311++G** basis set, the two τR_1 and τR_2 modes are predicted with A″ symmetry while the τR_3 mode is predicted with A′ symmetry in this medium. Remain skeletal modes were assigned to the weak Raman bands observed in the lower wavenumbers region, as it is detailed in Table 4.

5. Force field

Here, the harmonic force constants for ITFB in the two media were calculated by using both basis sets because they are parameters which are useful to describe the characteristics of the different bonds and, also because for this salt there were predicted ionic and of H bonds interactions by using the AIM analysis. In fact, the values calculated for ITFB are given in Table 5 compared with those reported for the furoyl salt [8]. In Fig. S10 the modifications that are present in those constants are observed when they change the medium and the basis set. First, we observed that the force constants values decrease in solution and with both basis sets, as it was also observed in the furoyl salt [8]. Then, the higher force constants values are observed for *f(νC═O)* in gas phase, having higher values

Table 4
Observed and calculated wavenumbers (cm^{-1}) and assignments for the most stable C4 conformer for the Potassum 2-isonicoinoyltrifluoroborate salt.

Experimental[a]			B3LYP 6-31G*[a]				B3LYP 6-311++G**[a]			
			Gas		PCM		Gas		PCM	
Modes	IR	Raman	SQM[b]	Assignment[a]	SQM[b]	Assignment[a]	SQM[b]	Assignment[a]	SQM[b]	Assignment[a]
A′ Symmetry										
1	3130vw	3132vw	3135	νC4–H10	3144	νC4–H10	3101	νC4–H10	3113	νC4–H10
2	3083vw	3060vs	3077	νC2–H9	3098	νC2–H9	3057	νC2–H9	3073	νC2–H9
3	3062w	3032w	3060	νC3–H7	3083	νC3–H7	3041	νC3–H7	3060	νC3–H7
4	3014vw	3001vw	3028	νC1–H8	3060	νC1–H8	3007	νC1–H8	3039	νC1–H8
5	1660vs	1660s	1621	νC11=O12	1596	νC11=O12	1603	νC11=O12	1572	νC11=O12
6		1582s	1580	νC3-C4	1576	νC3–C4	1560	νC3–C4	1553	νC3–C4
7	1566m	1567w	1565	βC2–H9	1566	βC2–H9	1548	βC2–H9	1548	βC2–H9
8	1459vw	1470vw	1452	βC4–H10	1452	βC4–H10	1437	βC4–H10	1435	βC1–H8
9	1432w	1434w	1439	βC1–H8	1443	βC1–H8	1421	βC1–H8	1427	βC3–H7
10	1298w	1270m	1307	νC1–N6	1304	νC1–N6	1294	νC1–N6	1290	νC1–N6
11	1230w	1231m	1210	νC4–C5	1210	νC4–C5	1193	νC4–C5	1194	νC4–C5
12	1128m		1181	βC3–H7	1175	βC3–H7	1167	βC3–H7	1164	βC4–H10
13		1141w	1159	νC5–C11	1164	νC5–C11	1144	νC5–C11	1153	νC5–C11
14	1106m	1126vw	1150	ν_aBF_3	1105	ν_aBF_3	1102	ν_aBF_3	1089	νC1–C2
15	1084m	1087w	1094	νC1–C2	1097	νC1–C2	1085	νC1–C2	1051	νC2–C3
16	1036vs	1044m	1049	νC2–C3	1050	νC2–C3	1037	νC2–C3	1034	βR_1
17	1005s		1024	βR_1	1027	βR_1	1016	βR_1	1002	γC1-H8
18		997s	981	γC1–H8	995	ν_aBF_3	972	γC4–H10	967	νC5–N6
19	891s	880vw	871	ν_sBF_3	868	ν_sBF_3	848	ν_sBF_3	906	ν_aBF_3
20	711w	713m	701	βR_2	702	βR_2	697	βR_2	732	τR_1
21	632m	638vw	627	βR_3	627	βR_3	627	βR_3	676	γC11–C5
22	582w		587	δ_sBF_3	582	δ_sBF_3	576	δ_sBF_3	627	βR_3
23	528vw		533	δ_aBF_3	532	δ_aBF_3	526	ρBF_3	570	δ_sBF_3
24	432vw		444	τR_3	444	νC11–B13	439	τR_3	441	τR_3
25		357w	377	βC11=O12	376	βC11=O12	372	βC11=O12	396	δ_aBF_3
26		289w	263	νC11–B13	269	βC5–C11	261	νC11–B13	369	βC11=O12
27		249w	243	ρBF_3	240	ρBF_3	240	βC5–C11	265	νC11–B13
28		193vvw	202	νF16–K17	171	νF16–K17	189	νF16–K17	225	$\rho'BF_3$
29		169vvw	168	δB13C11C5	155	δ B13C11C5	164	δB13C11C5	146	τwBF_3
30		118vvw	110	δK17B13C12	91	δ K17B13C12	104	δK17B13C12	143	νF14–K17
A″ Symmetry										
31		986vw	996	ν_aBF_3	998	γC1–H8	983	γC1–H8	1003	ν_aBF_3
32		972vw	979	νC5–N6	979	νC5–N6	970	νC5–N6	964	γC4–H10
33			971	γC4–H10	969	γC4–H10	917	ν_aBF_3	915	γC2–H9
34		901vw	903	γC3–H7	916	γC3–H7	901	γC3–H7	912	γC3–H7
35	789w		763	γC5–H11	766	γC5–H11	767	γC5–H11	843	ν_sBF_3
36	740m	748vw	735	τR_1	736	τR_1	733	τR_1	769	γC5–H11
37	674m	677vw	674	γC2–H9	678	γC2–H9	673	γC2–H9	698	βR_2
38	444vw	444w	448	βC5–C11	445	δ_aBF_3	441	δ_aBF_3	523	βC5–C11
39	418w	425vw	416	τR_2	412	τR_2	413	τ_2R	435	δ_aBF_3
40		398vw	404	δ_aBF_3	404	τR_3	394	δ_aBF_3	409	τR_2
41		223w	227	$\rho'BF_3$	221	$\rho'BF_3$	231	$\rho'BF_3$	236	ρBF_3
42		144vvw	145	τwBF_3	146	τwBF_3	146	τwBF_3	159	δB13C11C5
43		123vvw	127	νF14–K17	94	νF14–K17	113	νF14–K17	73	δK17B13C12
44			33	γC11–C5	51	τwC5–C11	35	γC11–C5	69	νF16–K17
45			26	τwC5–C11	18	γC11–C5	4	τwC5–C11	48	τwC5–C11

Abbreviations: ν, stretching; β, deformation in the plane; γ, deformation out of plane; wag, wagging; τ, torsion; β_R, deformation ring τ_R, torsion ring; ρ, rocking; τw, twisting; δ, deformation; a, antisymmetric; s, symmetric.
[a] This work.
[b] From scaled quantum mechanics force field.

in the ITFB salt than in FTFB. Besides, higher values of the *f(νBF₃)* force constants are also observed for ITFB than FTFB. Fig. S9 clearly evidences that the *f(νBF₃)* force constants in both media have higher values when the 6-31G* basis set is employed. In general, the change of the furane ring by pyridine one clearly generates an increase in the *f(νC=O) f(νBF₃)* force constants values and decrease the *f(νC-B), f(νC-C) f(δBF₃)* force constants in ITFB, as compared with FTFB.

6. Ultraviolet–visible spectrum

Here, TD-DFT calculations were employed together with the B3LYP/6-31G* and B3LYP/6-311++G** methods to predict the electronic spectra for ITFB in aqueous solution by using the Gaussian program [21]. The experimental UV–Visible spectrum for this salt in aqueous solution can be seen in Fig. 8 and it is compared with the corresponding predicted spectra for the salt and their anion by using both basis sets. In Table S6 the calculated and experimental wavelengths are shown for this salt compared with the bands observed in the same medium for the potassium 3-furoyltrifluoroborate salt [8]. Note that the positions of the bands corresponding to the salt are the same that for the anion, as expected because in solution that species is dissociated and, for this reason, the predicted bands for the anion are not presented. Experimentally, two very strong bands are observed at 238.0 and 258.0 nm, other very weak at 319.0 nm and a shoulder at 340.0 nm. Theoretically, for the salt in solution, three bands and a shoulder are predicted with both basis sets which by using the 6-31G* basis set are located at 240.1, 178.1, 148.6 and 131.9 nm, respectively and when the other basis set is used the positions of the bands change

Table 5
Comparison of scaled internal force constants for the most stable conformer of the Potassum 2-isonicoinoyltrifluoroborate salt in gas and aqueous solution phases by using two levels of theory.

Force constants	ITB[a]				FTB[b]			
	B3LYP/6-31G*		B3LYP/6311++G**		B3LYP/6-31G*		B3LYP/6311++G**	
	Gas	PCM	Gas	PCM	Gas	PCM	Gas	PCM
$f(\nu C{-}H)_R$	5.18	5.26	5.11	5.17	5.49	5.50	5.39	5.39
$f(\nu C{-}N)_R$	6.99	6.92	6.87	6.79				
$f(\nu C{-}C)_R$	6.47	6.52	6.33	6.38	6.84	6.83	6.68	6.66
$f(\nu C{=}O)$	10.60	10.21	10.43	9.93	10.07	9.77	9.81	9.41
$f(\nu C{-}B)$	2.86	2.92	2.81	2.87	2.94	2.97	2.89	2.92
$f(\nu BF_3)$	4.39	4.32	3.96	3.82	4.18	4.12	3.78	3.64
$f(\delta C{-}C{-}B)$	1.46	1.44	1.39	1.31	1.21	1.12	1.12	1.00
$f(\delta BF_3)$	1.22	1.24	1.18	1.12	1.28	1.24	1.24	1.18
$f(\rho BF_3)$	1.03	0.98	0.97	0.89	1.02	0.98	0.98	0.89

[a] This work.
[b] From Ref [8].

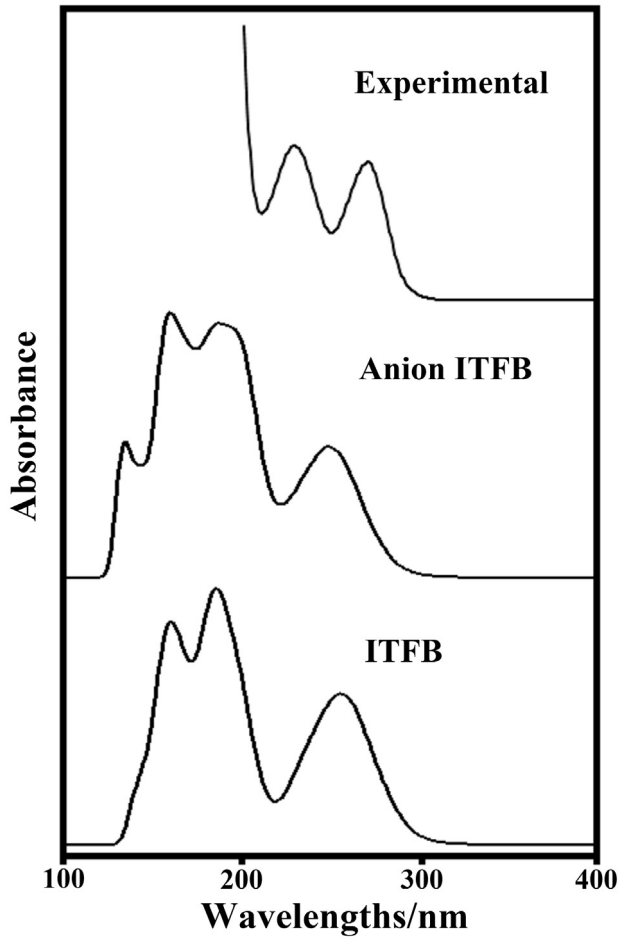

Fig. 8. Experimental UV–visible spectrum of the potassium 2-isonicotinoyltrifluorborate salt in aqueous solution compared with those predicted for the salt and their anion in the same media by using B3LYP/6-311++G** level of theory.

at 258.1, 184.9, 159.1 and 139.2 nm, respectively. In the UV–Vis spectrum of neutral pyridine the bands are observed at 200, 257 and 263 nm [41]. Hence, the effect of the incorporation of the fluoroborate group on the pyridine ring is the shifting of the bands towards higher wavelengths. In contrast, in the furoyl salt [8] the positions of the bands are shifted toward lower wavelengths (210, 223, 252 and 344 nm) in relation to the isonicotinol salt. Evidently, when the pyridine ring is replaced by the furane one the bands are clearly shifted toward lower wavelengths. Those groups of bands observed for this salt are assigned to $\pi \rightarrow \pi^*$ and $n \rightarrow \pi^*$ transitions attributed to the C=C and C=O groups present in the salt, as can be seen in Table S6 and, as predicted by NBO studies.

7. Conclusions

Here, the potassium 2-isonicotinoyltrifluorborate salt has been characterized by means of FT-IR and FT-Raman spectroscopies in the solid phase and by UV–Visible spectroscopy in aqueous solution. Four conformers, two with C_S symmetries and two with C_1 symmetries, were found in the potential energy surface but only one of them, named C4, presents the minimum energy and, for this reason, is the most stable. The molecular structures of C4 were theoretically determined in gas phase and in aqueous solution by using the B3LYP/6-31G* and B3LYP/6-311++G** methods. Two dimeric species were also optimized according to the layered architectures suggested for trifluoroborate potassium salts in the solid state. Two bands in the experimental Raman spectrum at 748 and 676 cm^{-1} and one band at 796 cm^{-1} clearly justify the presence of both dimers. The structure of the 2-isonicotinoyltrifluorborate anion was also studied because it is expected in solution. Then, very good correlations were observed when the experimental predicted UV–visible spectrum in aqueous solution was compared with those predicted for the salt and their anion. Both calculations predicted solvation energies for the salt in aqueous solution of −82.68 and −90.65 kJ/mol by using the B3LYP/6-31G* and B3LYP/6-311++G** methods, respectively. Here, it is observed that the change of furane by pyridine ring generates an increase in the solvation energies of the potassium 2-isonicotinoyltrifluorborate salt in relation to potassium 3-furoyltrifluoroborate salt. The study of the charges has revealed that there is an effect of the size of the basis set on the Mulliken charges while the AIM analyses suggest that the F–H and O–K interactions are also strongly dependent of the medium and the size of the basis sets. The bond orders for the F and K atoms evidence their higher ionic characteristics in solution with both basis sets. The NBO and AIM results clearly support higher stabilities of this salt in both media as compared with the potassium 3-furoyltrifluoroborate salt. The studies by using the frontier orbitals indicate that the change of furane by pyridine ring decreases the reactivity of this salt by using 6-31G* basis set but increases when the other one is employed. Another effect of changing furane by pyridine ring is observed in the increase of the $f(\nu C{=}O)$ and $f(\nu BF_3)$ force constants. In this study, the force fields for the salt in both media were reported together to their complete vibrational assignments and force constants by using both levels of theory.

Acknowledgements

This work was supported with grants from CIUNT Project 26/D207 (Consejo de Investigaciones, Universidad Nacional de Tucumán). The authors would like to thank Prof. Tom Sundius for his permission to use MOLVIB.

Appendix A. Supplementary data

Supplementary data related to this article can be found at https://doi.org/10.1016/j.molstruc.2018.02.098.

References

[1] A.M. Dumas, G.A. Molander, J.W. Bode, Amide-Forming ligation of acyltrifluoroborates and hydroxylamines in water, Angew. Chem. 51 (23) (2012) 5683–5686.

[2] I. Pusterla, J.W. Bode, The mechanism of the α-ketoacid-Hydroxylamine amide-forming ligation, Angew. Chem. 51 (2) (2012) 513–516.

[3] A.M. Dumas, G.A. Molander, J.W. Bode, Amide-Forming ligation of acyltrifluoroborates and hydroxylamines in water, Angew. Chem. 124 (23) (2012) 5781–5784.

[4] A.M. Dumas, G.A. Molander, J.W. Bode, Amide-Forming ligation of acyltrifluoroborates and hydroxylamines in water, Chemin. Abstr. 43 (44) (2012) 5683–5686.

[5] H. Noda, G. Erős, J.W. Bode, Rapid ligations with equimolar reactants in water with the potassium acyltrifluoroborate (KAT) amide formation, J. Am. Chem. Soc. 136 (15) (2014) 5611–5614.

[6] H. Noda, J.W. Bode, Synthesis of chemically and configurationally stable monofluoro acylboronates: effect of ligand structure on their formation, properties, and reactivities, J. Am. Chem. Soc. 137 (11) (2015) 3958–3966.

[7] H. Noda, J.W. Bode, Synthesis and reactivities of monofluoro acylboronates in chemoselective amide bond forming ligation with hydroxylamines, Chemin. Abstr. 47 (8) (2016) 3958–3966.

[8] M.A. Iramain, L. Davies, S.A. Brandán, FTIR, FT-Raman and UV-visible spectra of Potassium 3-furoyltrifluoroborate, J. Mol. Struct. 1158 (2018) 245–254.

[9] A.D. Becke, Density functional thermochemistry. III. The role of exact exchange, J. Chem. Phys. 98 (1993) 5648–5652.

[10] C. Lee, W. Yang, R.G. Parr, Development of the Colle-Salvetti correlation-energy formula into a functional of the electron density, Phys. Rev. B 37 (1988) 785–789.

[11] S. Miertus, E. Scrocco, J. Tomasi, Electrostatic interaction of a solute with a continuum, Chem. Phys. 55 (1981) 117–129.

[12] J. Tomasi, J. Persico, Molecular interactions in solution: an overview of methods based on continous distributions of the solvent, Chem. Rev. 94 (1994) 2027–2094.

[13] A.V. Marenich, C.J. Cramer, D.G. Truhlar, Universal solvation model based on solute electron density and a continuum model of the solvent defined by the bulk dielectric constant and atomic surface tensions, J. Phys. Chem. B 113 (2009) 6378–6396.

[14] a) G. Rauhut, P. Pulay, Transferable scaling factors for density functional derived vibrational force fields, J. Phys. Chem. 99 (1995) 3093–3099;
b) G. Rauhut, P. Pulay, J. Phys. Chem. 99 (1995) 14572.

[15] T. Sundius, Scaling of ab-initio force fields by MOLVIB, Vib. Spectrosc. 29, 89–95.

[16] E.D. Gledening, J.K. Badenhoop, A.D. Reed, J.E. Carpenter, F.F. Weinhold, NBO 3.1, Theoretical Chemistry Institute, University of Wisconsin, Madison, WI, 1996.

[17] F. Biegler-Köning, J. Schönbohm, D. Bayles, AIM2000; a program to analyze and visualize atoms in molecules, J. Comput. Chem. 22 (2001) 545.

[18] R.G. Parr, R.G. Pearson, Absolute hardness: companion parameter to absolute electronegativity, J. Am. Chem. Soc. 105 (1983) 7512–7516.

[19] J.-L. Brédas, Mind the gap!, Mater. Horiz. 1 (2014) 17–19.

[20] A.B. Nielsen, A.J. Holder, GaussView, User's Reference, GAUSSIAN, Inc., Pittsburgh, PA, USA, 2000-2003.

[21] M.J. Frisch, G.W. Trucks, H.B. Schlegel, G.E. Scuseria, M.A. Robb, J.R. Cheeseman, G. Scalmani, V. Barone, B. Mennucci, G.A. Petersson, H. Nakatsuji, M. Caricato, X. Li, H.P. Hratchian, A.F. Izmaylov, J. Bloino, G. Zheng, J.L. Sonnenberg, M. Hada, M. Ehara, K. Toyota, R. Fukuda, J. Hasegawa, M. Ishida, T. Nakajima, Y. Honda, O. Kitao, H. Nakai, T. Vreven, J.A. Montgomery Jr., J.E. Peralta, F. Ogliaro, M. Bearpark, J.J. Heyd, E. Brothers, K.N. Kudin, V.N. Staroverov, R. Kobayashi, J. Normand, K. Raghavachari, A. Rendell, J.C. Burant, S.S. Iyengar, J. Tomasi, M. Cossi, N. Rega, J.M. Millam, M. Klene, J.E. Knox, J.B. Cross, V. Bakken, C. Adamo, J. Jaramillo, R. Gomperts, R.E. Stratmann, O. Yazyev, A.J. Austin, R. Cammi, C. Pomelli, J.W. Ochterski, R.L. Martin, K. Morokuma, V.G. Zakrzewski, G.A. Voth, P. Salvador, J.J. Dannenberg, S. Dapprich, A.D. Daniels, Ö. Farkas, J.B. Foresman, J.V. Ortiz, J. Cioslowski, D.J. Fox, Gaussian 09, Revision D.01, Gaussian, Inc., Wallingford CT, 2009.

[22] F. Chain, M.F. Ladetto, A. Grau, C.A.N. Catalán, S.A. Brandán, Structural, electronic, topological and vibrational properties of a series of N-benzylamides derived from Maca (Lepidium meyenii) combining spectroscopic studies with ONION calculations, J. Mol. Struct. 1105 (2016) 403–414.

[23] D. Romani, S.A. Brandán, M.J. Márquez, M.B. Márquez, Structural, topological and vibrational properties of an isothiazole derivatives series with antiviral activities, J. Mol. Struct. 1100 (2015) 279–289.

[24] F. Chain, E. Romano, P. Leyton, C. Paipa, C.A.N. Catalán, M.A. Fortuna, S.A. Brandán, An experimental study of the structural and vibrational properties of sesquiterpene lactone cnicin using FT-IR, FT-Raman, UV–visible and NMR spectroscopies, J. Mol. Struct. 1065–1066 (2014) 160–169.

[25] Radosław Kamiński, Katarzyna N. Jarzembska, Marek Dąbrowski, Krzysztof Durka, Marcin Kubsik, Janusz Serwatowski, Krzysztof Woźniak, Finding rules governing layered architectures of trifluoroborate potassium salts in the solid state, Cryst. Growth Des. 16 (3) (2016) 1687–1700.

[26] Aurelia Falcicchio, Sten O. Nilsson Lill, Filippo M. Perna, Antonio Salomone, Donato I. Coppi, Corrado Cuocci, Dietmar Stalked, Vito Capriati, Organotrifluoroborates as attractive self-assembling systems: the case of bifunctional dipotassium phenylene-1,4-bis(trifluoroborate), Dalton Trans. 44 (2015) 19447–19450.

[27] Christopher M. Bateman, Lev N. Zakharov, Eric R. Abbey, Crystal structure of triphenylphosphoniummethylenetrifluoroborate, Acta Crystallogr. E73 (2017) 1140–1142.

[28] H.A. Höppe, K. Kazmierczak, E. Romano, S.A. Brandán, A structural and vibrational study on the first potassium borosulfate, $K_5[B(SO_4)_4]$ by using the FTIR-Raman and DFT calculations, J. Mol. Struct. 1037 (2013) 294–300. ISSN: 0022-2860.

[29] E. Romano, L. Davies, S.A. Brandán, Structural and vibrational properties of zinc difluoromethanesulfinate. A study combining the FTIR and Raman spectra with ab-initio calculations, J. Mol. Struct. 1044 (2013) 144–151.

[30] G. Berionni, B. Maji, P. Knochel, H. Mayr, Nucleophilicity parameters for designing transition metal-free C–C bond forming reactions of organoboron compounds, Chem. Sci. 3 (2012) 878–882.

[31] P. Ugliengo, MOLDRAW Program, University of Torino, Dipartimento Chimica IFM, Torino, Italy, 1998.

[32] D. Romani, I. Salas Tonello, S.A. Brandán, Influence of atomic bonds on the properties of the laxative drug sodium picosulphate, Heliyon 2 (2016), e00190.

[33] D. Mootz, H.-G. Wussow, Crystal structures of pyridine and pyridine trihydrate, J. Chem. Phys. 75 (3) (1981) 1517–1522.

[34] Julio Zukerman Schpector, Rafael C. Guadagnin, Hélio A. Stefani, Lorenzo do Canto Visentin, Potassium trifluoro[(*Z*)-3-methoxyprop-1-enyl]borate, Acta Crystallogr. Sect. E E64 (2008) 1525–1526.

[35] Julio Zukerman-Schpector, Rafael C. Guadagnin, Hélio A. Stefani, Lorenzo do Canto Visentin, Potassium trifluoro[(*Z*)-3-(oxan-2-yloxy)prop-1-en-1-yl] borate monohydrate, Acta Crystallogr. Sect. E E65 (2009) 192–194. ISSN 1600-5368.

[36] R.F.W. Bader, Atoms in Molecules. A Quantum Theory, Oxford University Press, Oxford, 1990. ISBN: 0198558651.

[37] G. Keresztury, S. Holly, G. Besenyei, J. Varga, A.Y. Wang, J.R. Durig, Vibrational spectra of monothiocarbamates-II. IR and Raman spectra, vibrational assignment, conformational analysis and *ab initio* calculations of *S*-methyl-*N*,*N*-dimethylthiocarbamate, Spectrochim. Acta 49A (1993) 2007–2026.

[38] D. Romani, S.A. Brandán, Structural, electronic and vibrational studies of two 1,3-benzothiazole tautomers with potential antimicrobial activity in aqueous and organic solvents. Prediction of their reactivities, Comput. Theor. Chem. 1061 (2015) 89–99.

[39] M.J. Márquez, M.B. Márquez, P.G. Cataldo, S.A. Brandán, A comparative study on the structural and vibrational properties of two cyanopyridine derivatives with potentials antimicrobial and anticancer activities, OJSTA 4 (2015) 1–19.

[40] M. Minteguiaga, E. Dellacassa, M.A. Iramain, C.A.N. Catalán, S.A. Brandán, A structural and spectroscopic study on carquejol, a relevant constituent of the medicinal plant Baccharis trimera (Less.) DC. (Asteraceae), J. Mol. Struct. 1150 (2017) 8–20.

[41] I. Kaljurand, T. Rodima, I. Leito, I.A. Koppel, R.J. Schwesinger, Self-consistent spectrophotometric basicity scale in acetonitrile covering the range between pyridine and DBU, Org. Chem. 65 (2000) 6202–6208.